Supporting Information

1. Supporting experimental details

1.1 Materials

Alizarin red S ($C_{14}H_7NaO_7S \cdot H_2O$), hydrofluoric acid (HF, 40 wt.%), hydrogen peroxide (H_2O_2, 30 wt.%), potassium hydroxide (KOH, 90%), 2,2,6,6-tetramethylpiperidine-1-oxyl ($C_9H_{18}NO$), and thioanisole (C_7H_8S) were purchased from Alfa Aesar. Degussa P25 was purchased from Shanghai Haiyi Co. All reagents were used as received without further purification.

1.2 Synthesis of potassium titanate nanowires (KTNWs)

Typically, KOH (44.8 g) and P25 (2 g) were successively added into distilled water (80 mL),[1] and after continuous stirring, the obtained white suspension was transferred to Teflon-lined stainless-steel autoclave. After holding at 200 °C for 24 h, white precipitates were collected by centrifugation. The obtained white precipitates were washed with distilled water and ethanol three times respectively, and then dried at 60 °C to obtain KTNWs.

1.3 Preparation of solid TiO_2 tetrakaidecahedron (STT):

STT were synthesized by a one-step hydrothermal process by using KTNWs as the precursor. Typically, KTNWs (0.025 g) was dispersed in distilled water (27 mL), H_2O_2 (3 mL; 30%), and HF (0.106 mL, 40 wt%). The suspension was transferred to a Teflon-lined autoclave and heated at 180 °C for 12 h. After the autoclave cooled to room temperature, samples were collected by centrifugation, washed with distilled water and ethanol, and dried at 60 °C in an oven.

1.4 Synthesis of hollow TiO_2 tetrakaidecahedron (HTT)

Typically, the obtained STT (0.01g) were dispersed in distilled water (19.88 mL) and HF (0.12 mL,40 wt%) under intense ultrasonic treatment. The resulting solution was then transferred into a 50 mL Teflon-lined autoclave and heated at 180 °C for 12 h. After the autoclave cooled to room temperature, samples were collected by centrifugation, washed with distilled water and ethanol, and dried at 60 °C in an oven.

1.5 Synthesis of solid TiO_2 cuboctahedron with wholly {101} and {001} faceted surfaces

(STC)

The solid TiO_2 cuboctahedron with wholly {101} and {001} faceted surfaces was synthesized through a hydrothermal reaction. First, a 0.015 M titanium tetrachloride ($TiCl_4$) solution was prepared by dissolving $TiCl_4$ into 2 M HCl solutions under strong stirring in an ice water bath. Then, a 60 mL of $TiCl_4$ solution with 2 M HCl was added to a Teflon-lined autoclave with 0.045 M sodium fluoride (NaF), and kept at 160 ^oC for 12 h. After the autoclave cooled to room temperature, samples were collected by centrifugation, washed with distilled water and ethanol, and dried at 60 ^oC in an oven.

1.6 Photocatalytic tests for the hydrogen evolution

The photocatalytic reaction was carried out in a gas-closed system with a quartz test tube. In a typical experiment, the photocatalyst (10 mg), chloroplatinic acid solution (100 μL, 0.02 M), and benzyl alcohol (100 μL) were added into deionized water (2 mL). The mixture solution was sonicated for 5 min to form a suspension. Then, N_2 was bubbled in the suspension for 30 min. After making the quartz test tube in a vacuum state, the suspension was irradiated with a 500 W Hg lamp (PLS-LAM500). The average light density was ca. 3.85 mW/cm^2 and the irradiation area was 2.46 cm^2. The amount of hydrogen produced was measured with a gas chromatography (Shanghai Techcomp Instrument Ltd, GC-7900, TCD, molecular sieve 5A 60-80 mesh) using N_2 as a carrier gas.

1.7 Photocatalytic tests for the oxidation of sulfides

In a typical reaction, the photocatalyst (10 mg), thioanisole (0.1 mmol), and TEMPO (0.02 mmol) were added to CH_3OH (3 mL). The mixture solution was stirred and irradiated by Hg lamp 500 W under atmosphere at room temperature for 24 h. ^1H NMR was employed to determine the yield. To carry out recycling reactions, the photocatalyst was recycled by centrifuging at 8000 rpm for 3 min and washed by ethanol three times. Finally, the recycled catalyst was dried in vacuum at 60 °C overnight.

1.8 Photocatalytic tests for the cross-dehydrogenative coupling (CDC) reaction

The photocatalyst (5 mg), tetrahydroisoquinolines (0.05 mmol) and indoles (0.1 mmol) were added into CD_3CN (1 mL). The mixture solution was stirred and irradiated by mercury lamp under atmosphere at room temperature for 12 h. The yield of the product was characterized by ^1H NMR spectra.

1.9 Photoelectrochemical measurements

Photoelectrochemical experiments were measured in the three-electrode quartz cell. The Pt plate was selected as the counter electrode, the reference electrode was $Hg/HgCl_2$ electrode, and the corresponding working electrode was obtained on the FTO glass. In order to obtain a slurry, the product (10 mg) was ultrasonicated in ethanol solution (0.2 mL). The slurry was then spread onto FTO glass with the other side protected by using Scotch tape. After drying in air, the Scotch tape was unstuck. In order to improve the adhesion, the obtained working electrode with the area about 2.5 cm^2 was dried at 300 °C for 180 min. In the three-electrode cell, the 0.025M NaH_2PO_4 and 0.025M Na_2HPO_4 standard buffer solution (25 ºC, pH = 6.864), 0.1M Na_2SO_4 solution and 0.1M NaOH solution were selected as the electrolyte respectively, without adding any additive. The study was performed on open circuit potential conditions. A 300 W Xe arc lamp system was used to provide visible light irradiation source. The CHI-760E workstation was used to measure the electrochemical impedance spectroscopy (EIS). The LSV technique was used to obtain cathodic polarization curves.

1.10 Photoluminescence (PL) measurements

The PL measurements of all HTT, STC and STC were unified as follows: samples (2 mg) were pressed as uniform circles with the diameter of about 1 cm, so that the quartz plate accessory was fully covered to ensure the unified illumination condition.

1.11 Calculation details

All theoretical calculations were carried out in the Cambridge Sequential Total Energy Package (CASTEP) code, based on plane-wave pseudopotential method.[2] The exchange-correlation effects were described by the local density approximation (LDA).[3] The electron-ion interactions were treated by ultrasoft pseudopotential.[4] Γ and 2×2×1 points were used as a Morkhost-Pack mesh[5] of k-points for geometry optimization and calculating electronic properties. The self-consistent convergence accuracy, the convergence criterion for the force between atoms, and the maximum displacement were set at 2×10^{-5} eV/atom, 3.0×10^{-2} eV/Å, and 2×10^{-3} Å, respectively. The cutoff energy was set to 340 eV.

The adsorption energy of H_2O molecule adsorbed on TiO_2 surface was calculated as

$$E_{ad} = E_{total} - E_{surface} - E_{H_2O}$$

where E_{total}, $E_{surface}$ and E_{H_2O} represented the total energy of the adsorbed H_2O molecule on TiO_2 surface, TiO_2 surface, and H_2O molecule, respectively.

The adsorption energy of O_2 molecule adsorbed on TiO_2 surface was calculated as

$$E_{ad} = E_{total} - E_{surface} - E_{O_2}$$

where E_{total}, $E_{surface}$ and E_{O_2} represented the total energy of the adsorbed O_2 molecule on TiO_2 surface, TiO_2 surface, and O_2 molecule, respectively.

The Gibbs free-energy of the intermediate adsorbed H* was calculated as

$$\Delta G_{H^*} = \Delta E_{H^*} + \Delta E_{ZPE} - T\Delta S$$

where ΔE_{H^*} was the hydrogen chemisorption energy, and ΔE_{ZPE} was the difference corresponding to the zero point energy between the adsorbed state and the gas phase. As the vibrational entropy of H* in the adsorbed state is small, the entropy of adsorption of 1/2 H_2 is $\Delta S_H \approx -{}^1/_2\, S^0_{H_2}$, where $S^0_{H_2}$ was the entropy of H_2 in the gas phase at the standard conditions.

Therefore, the overall corrections were taken as in

$\Delta G_{H^*} = \Delta E_{H^*} + 0.24\ eV$

2. Supplementary results

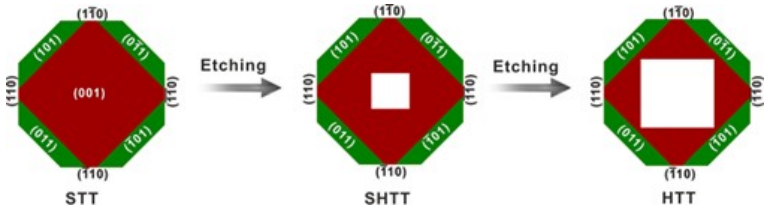

Figure S1 Schematic presentation showing the synthetic process of monodispersed hollow TiO_2 tetrakaidecahedron.

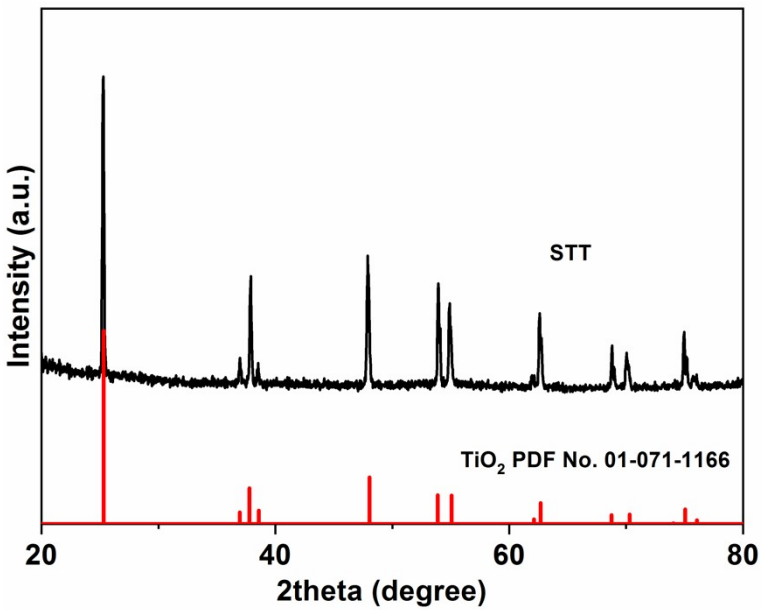

Figure S2 Powder XRD pattern of solid TiO_2 tetrakaidecahedron (STT).

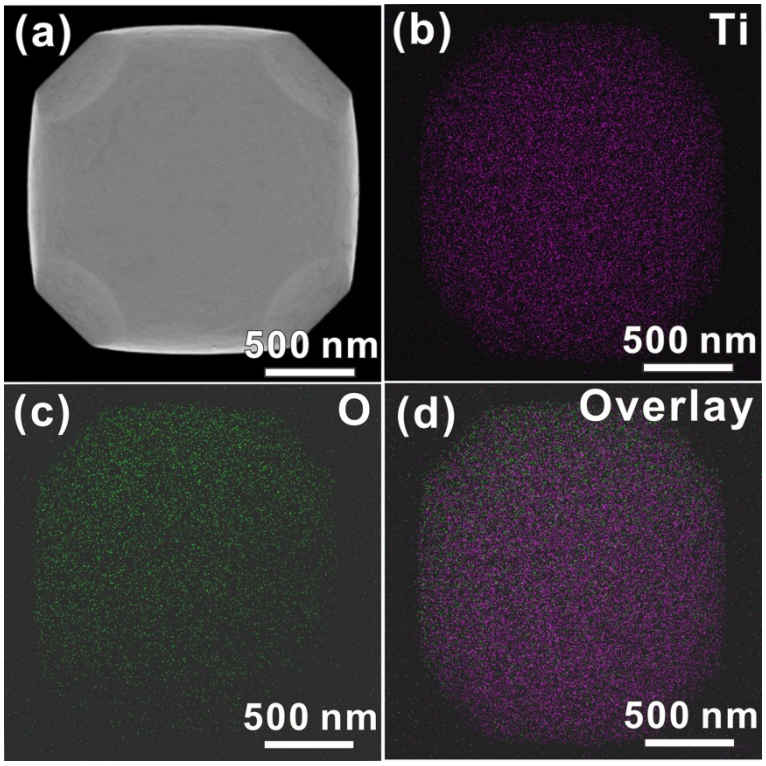

Figure S3 EDX mapping of solid TiO_2 tetrakaidecahedron (STT).

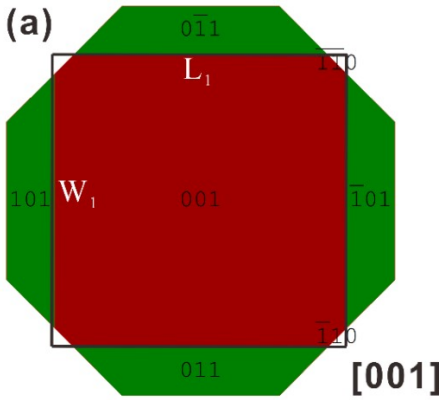

$$S_{\{001\}} \approx L_1 \times W_1 \times 2$$

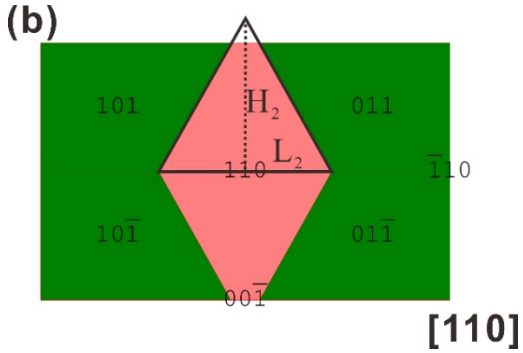

$$S_{\{110\}} \approx (L_2 \times H_2) / 2 \times 2 \times 4$$

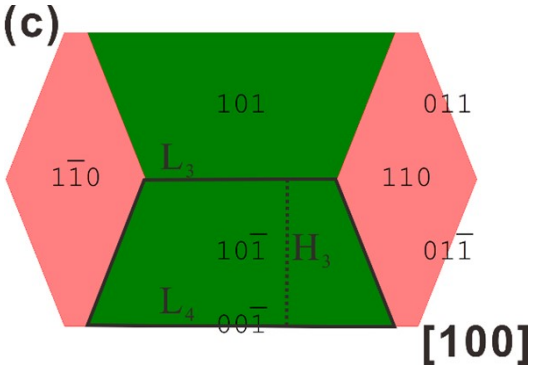

$$S_{\{101\}} \approx (L_3 + L_4) / 2 \times H_3 \times 2 \times 4;$$

$$S_{\{101\}}\% = S_{\{101\}} / [S_{\{001\}} + S_{\{110\}} + S_{\{101\}}] = 43\%$$

$$S_{\{001\}}\% = S_{\{001\}} / [S_{\{001\}} + S_{\{110\}} + S_{\{101\}}] = 37\%$$

$$S_{\{110\}}\% = S_{\{110\}} / [S_{\{001\}} + S_{\{110\}} + S_{\{101\}}] = 20\%$$

Figure S4 (a-c) Models of STT projected from different directions.

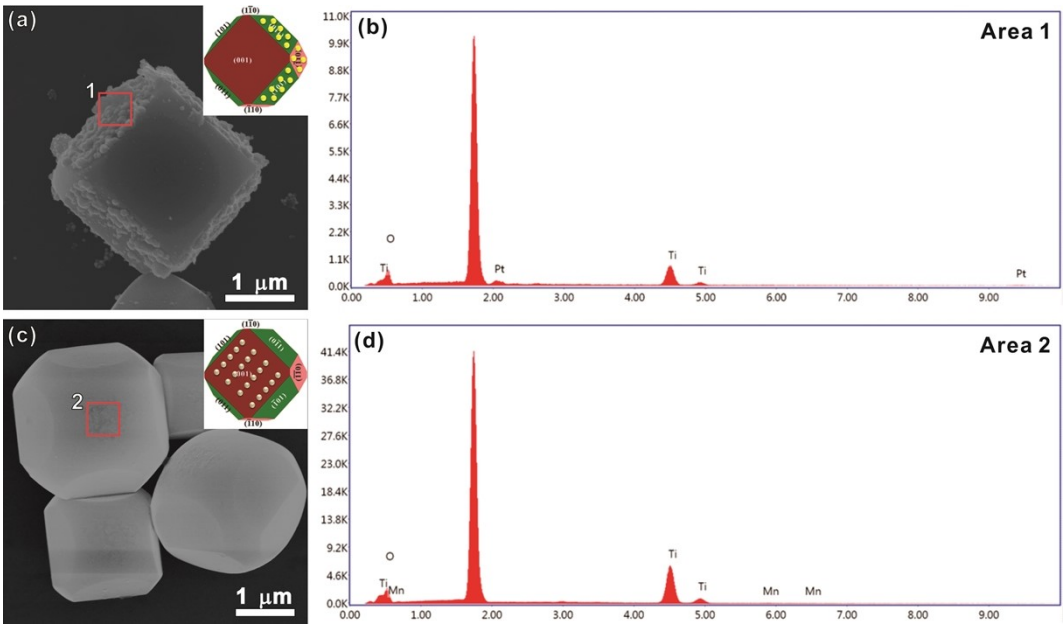

Figure S5 SEM images of STT with Pt deposition (a) and the EDS spectra of selected area 1 (b), SEM images of STT with MnO_x deposition (c) and the EDS spectra of selected area 2 (d).

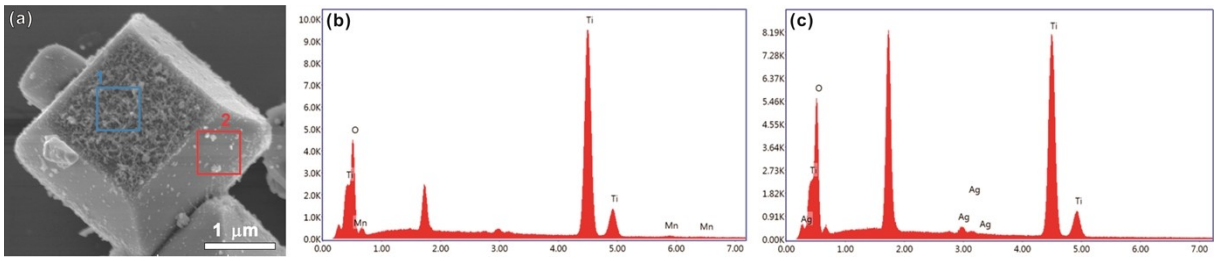

Figure S6 (a) SEM image of STT with Ag and MnO_x co-deposition. The EDS spectra of the selected area 1 (b) and area 2 (c).

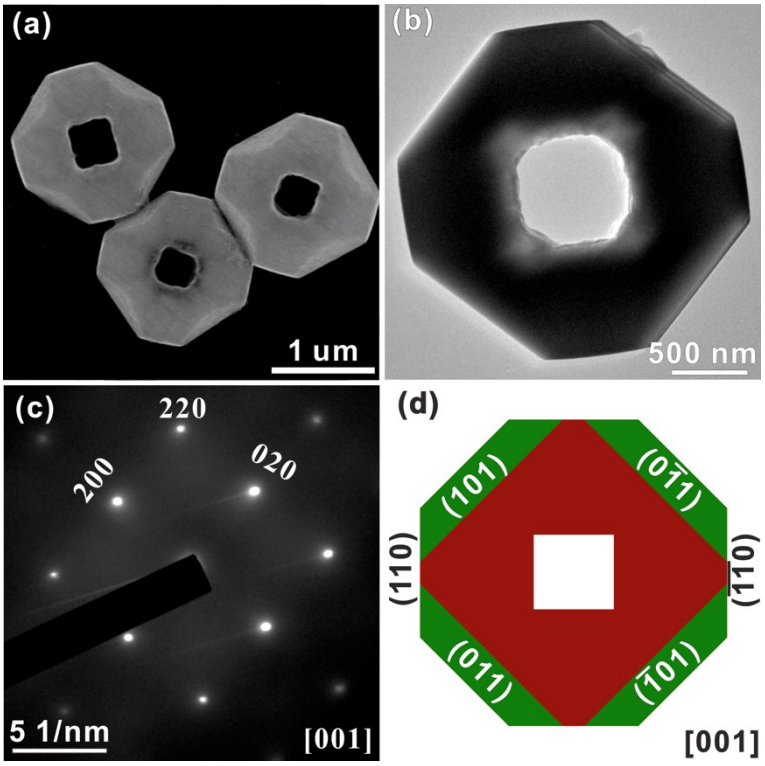

Figure S7 (a) Typical SEM images of SHTT. (b) Typical TEM images of an individual SHTT projected from the [001] directions. (c) Corresponding SAED patterns for SHTT projected from the [001] directions. (d) Models of SHTT viewed along the [001] directions.

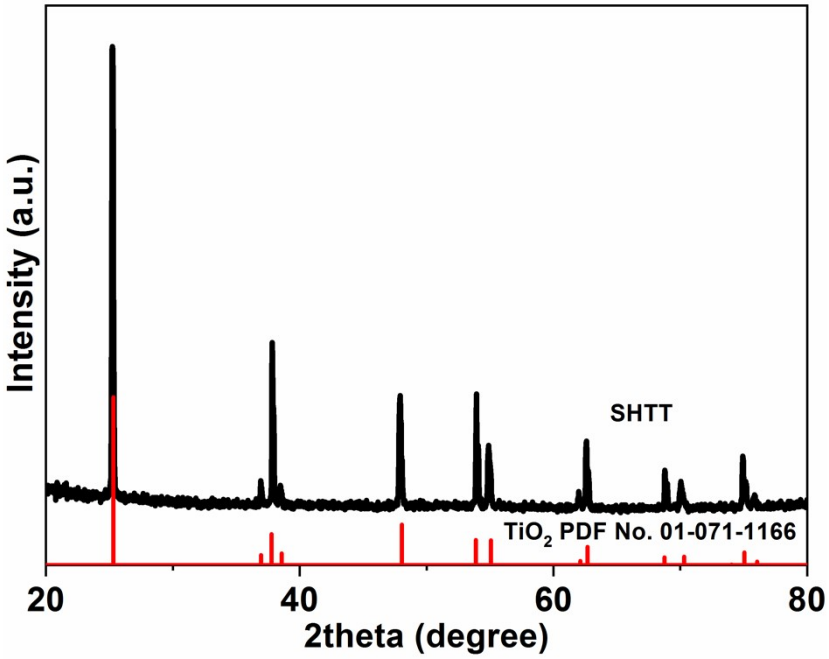

Figure S8 Powder XRD pattern of small hollow TiO_2 tetrakaidecahedron (SHTT).

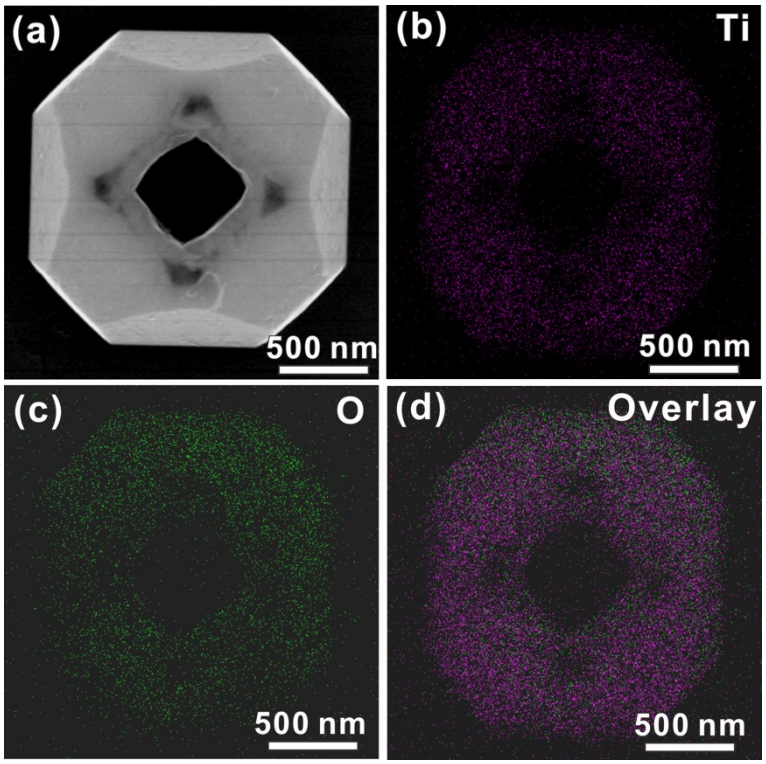

Figure S9 EDX mapping of small hollow TiO_2 tetrakaidecahedron (SHTT).

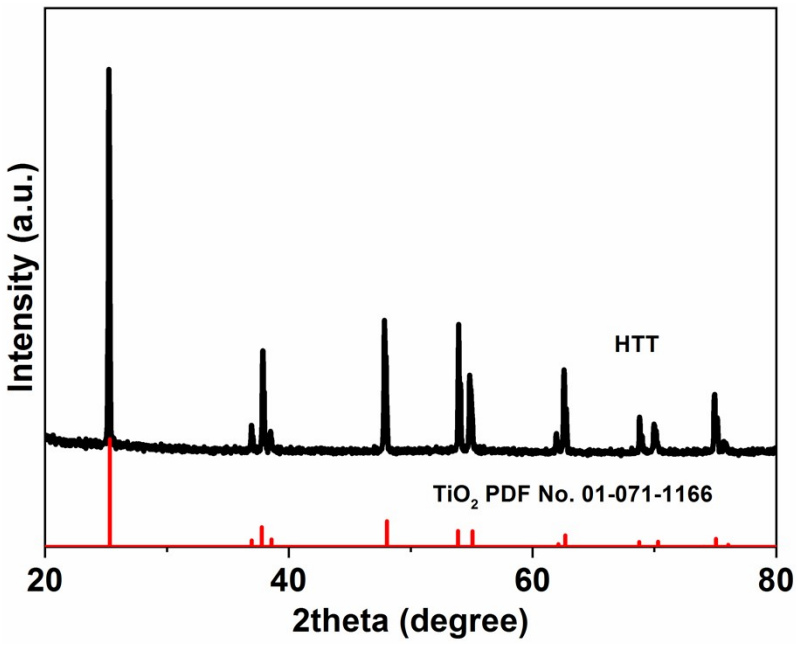

Figure S10 Powder XRD pattern of hollow TiO_2 tetrakaidecahedron (HTT).

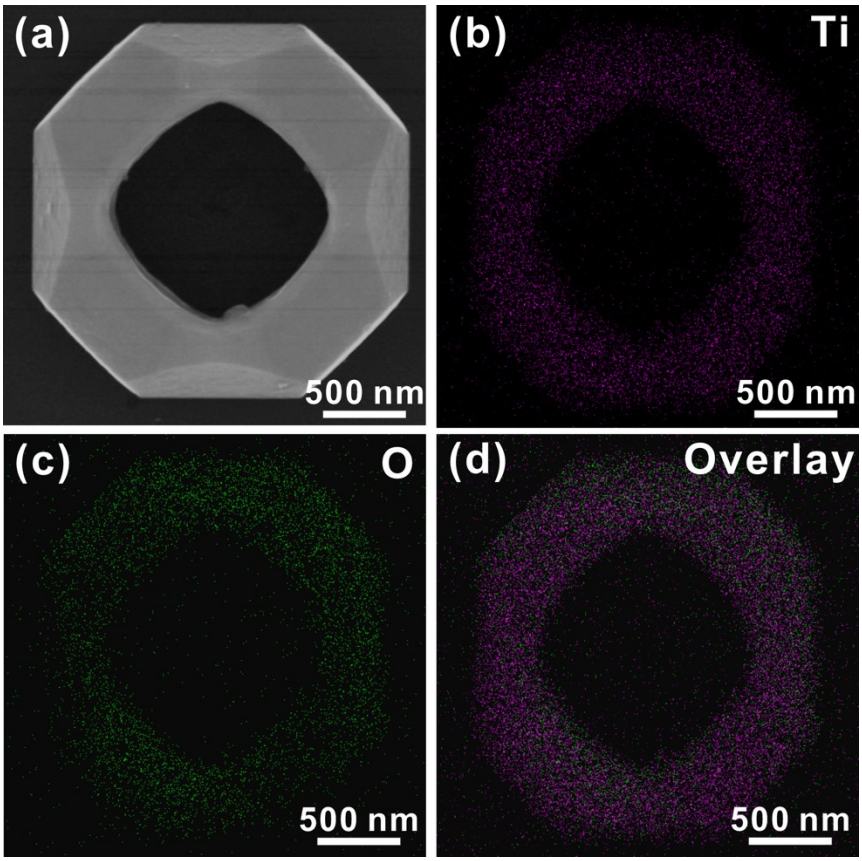

Figure S11 EDX mapping of hollow TiO_2 tetrakaidecahedron (HTT).

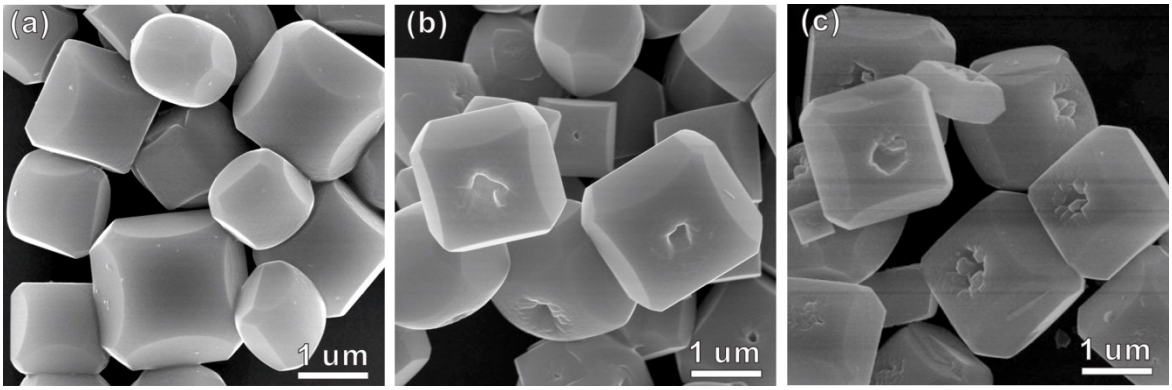

Figure S12 SEM images of STT etched at 180 °C for 12 h in (a) HCl solution, (b) HCl and NaF mixed solution, and (c) NaF solution, respectively.

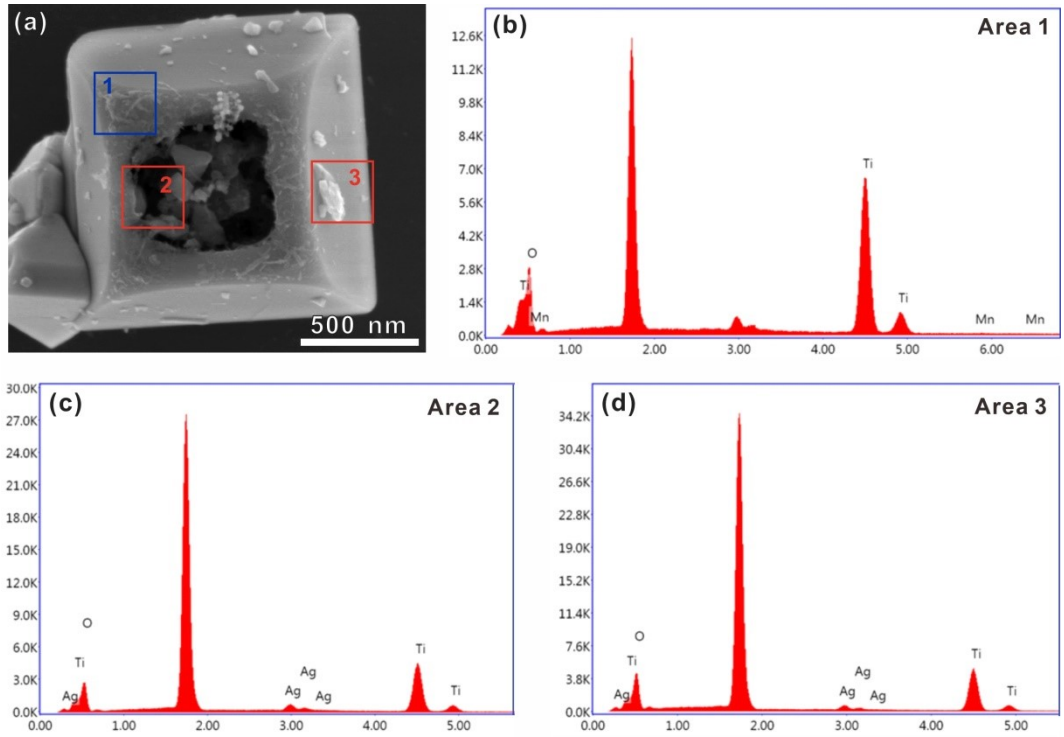

Figure S13 (a) SEM image of HTT with Ag and MnO_x co-deposition. The EDS spectra of the selected area 1 (b), area 2 (c) and area 3 (d).

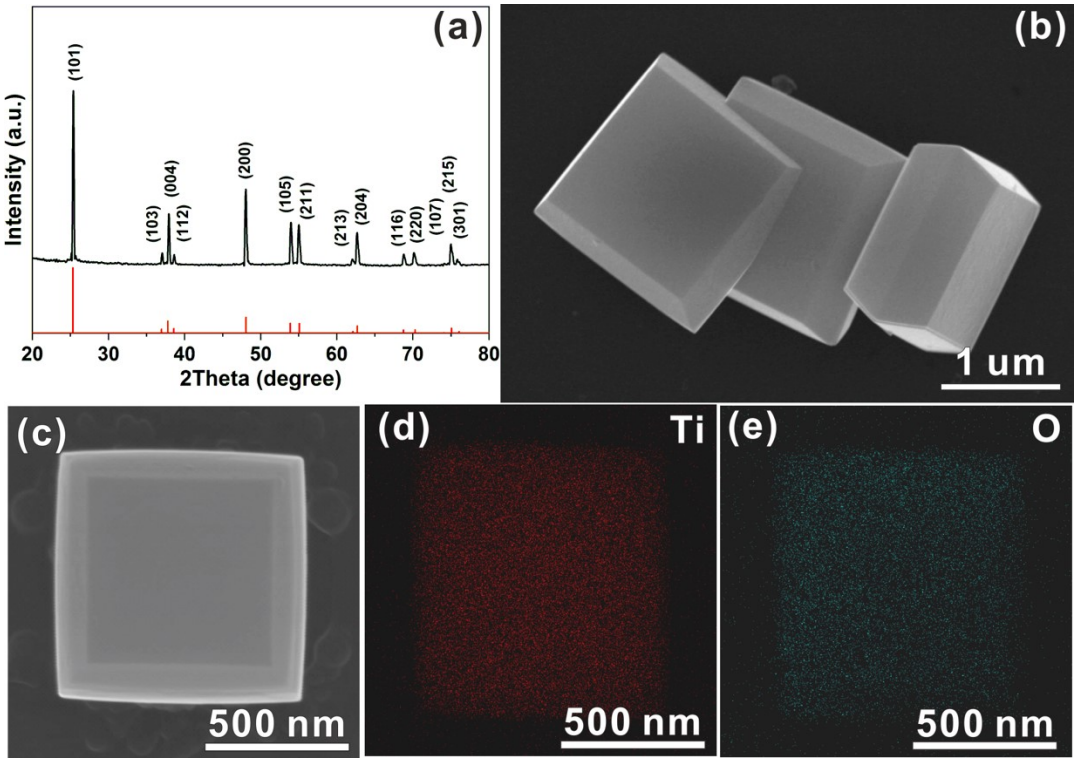

Figure S14 (a) Powder XRD pattern, (b,c) SEM images, and (d,e) EDX mapping of solid TiO_2 cuboctahedron composed of {101} and {001} facets (STC).

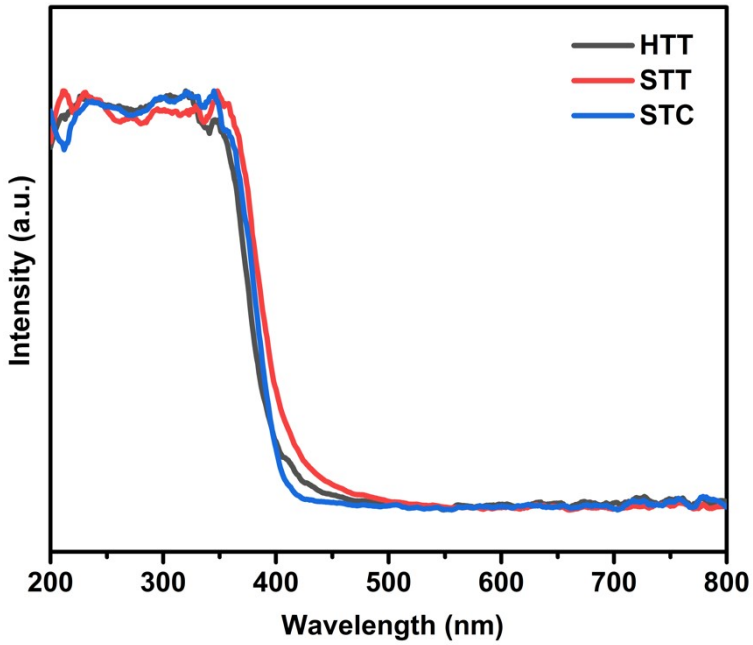

Figure S15 UV-vis absorption spectra of STC, STT and HTT.

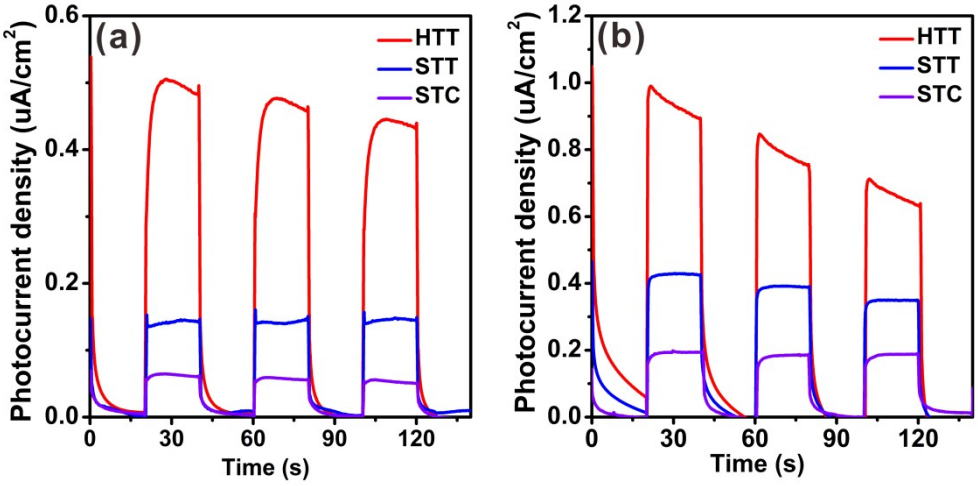

Figure S16 Photocurrent density of STC, STT and HTT measured at 0.2V versus Hg/Hg_2Cl_2 in Na_2SO_4 electrolyte (a) and NaOH electrolyte (b).

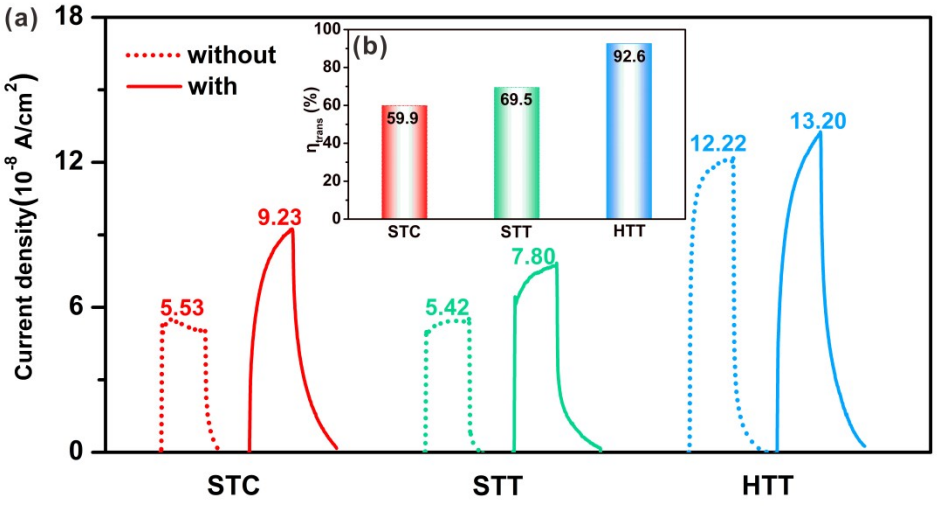

Figure S17 (a) Photocurrent density of STC, STT and HTT with and without electron scavenger KIO_3 under illumination, and (b) surface charge transfer efficiency of STC, STT and HTT.

Due to the existence of electron scavenger KIO_3, the η_{trans} approximately equals to 100%. The photocurrent follows the equations (eq. (1) and (2)):

$$J_{H_2O} = J_{max} \cdot \eta_{abs} \cdot \eta_{sep} \cdot \eta_{trans} \qquad (1)$$

$$J_{KIO_3} = J_{max} \cdot \eta_{abs} \cdot \eta_{sep} \cdot 100\% \qquad (2)$$

Here, J_{H_2O} and J_{max} represent for the measured and the theoretical maximum photocurrent without electron scavenger, respectively. η_{abs} and η_{sep} are the light absorption efficiency and charge separation efficiency inside the photoanode, respectively. η_{abs} and η_{sep} are the same for both J_{H_2O} and J_{KIO_3}. pH and other parameters are not changed upon adding KIO_3. Thus, the η_{trans} can be obtained by comparing the potocurrent from water and KIO_3 reduction (eq. (3)).

$$\eta_{trans} = J_{H_2O} / J_{KIO_3} \qquad (3)$$

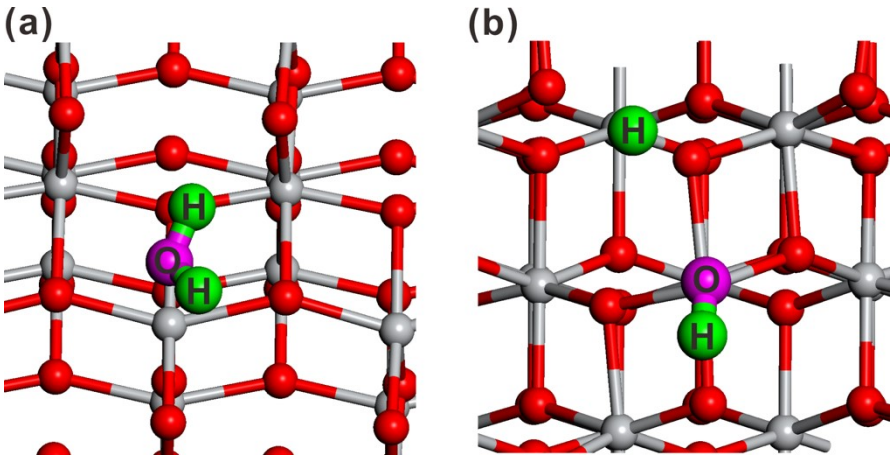

Figure S18 Optimized structural models of dissociative H_2O adsorbed on (a) (101) and (b) (110) surface.

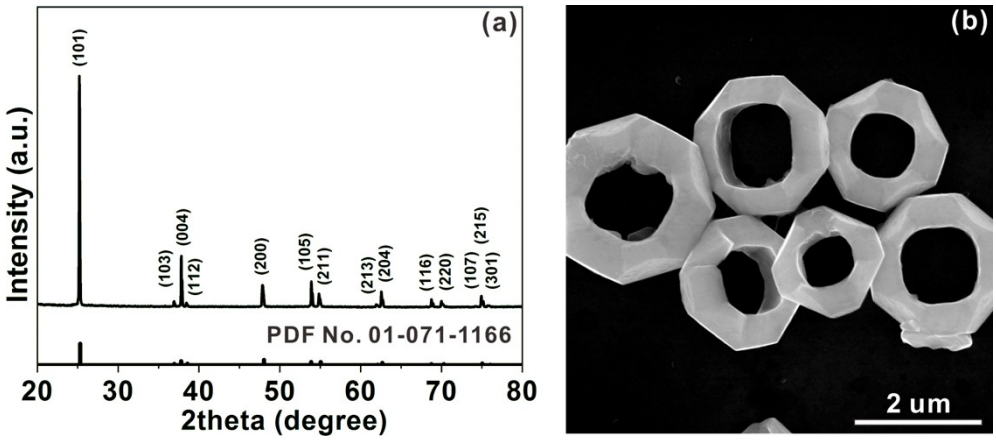

Figure S19 (a) Powder XRD pattern and (b) SEM image of HTT after photocatalytic reaction.

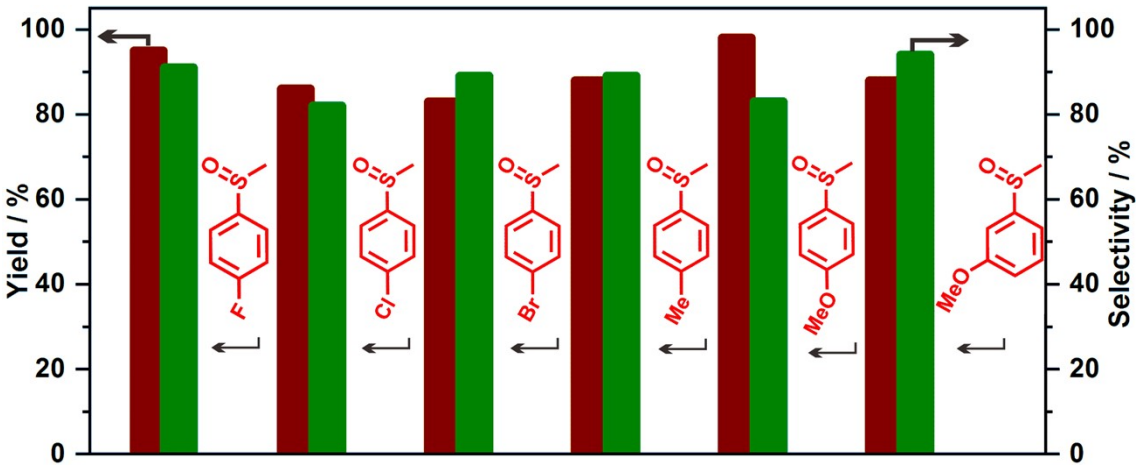

Figure S20 Scope of Hg lamp-induced selective oxidation of sulfides to sulfoxides in air on HTT.

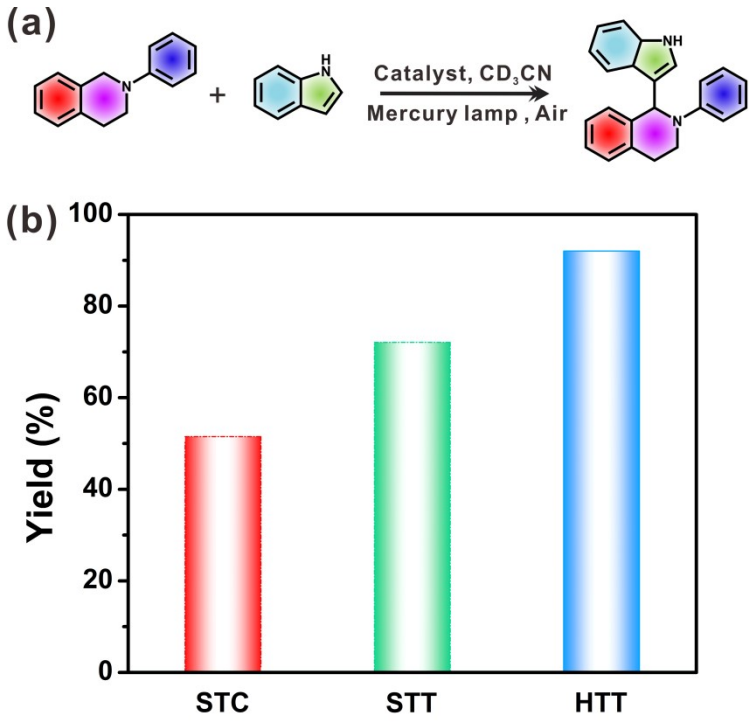

Figure S21 (a) Photocatalytic equation and conditions for the CDC reaction, and (b) product yield with HTT, STT and STC as photocatalysts.

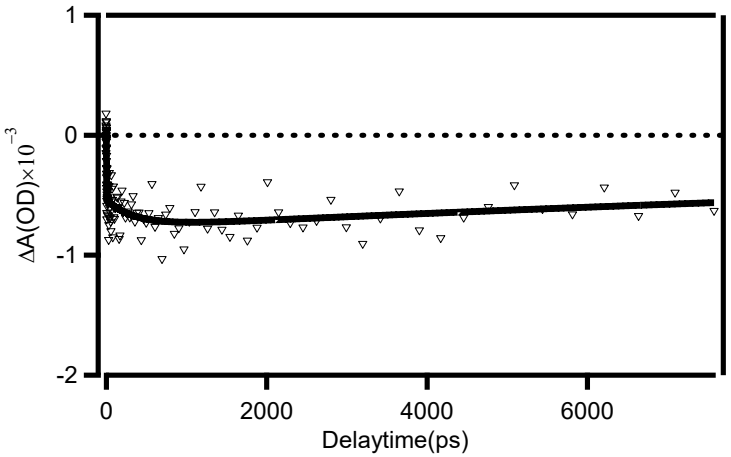

Figure S22 Kinetic traces of STT at 770 nm.

Table S1 Fitting parameters to the Nyquist plots for HTT, STT and STC.

	R_s (Ω)	R_{CT} (Ω)	CPE-T	CPE-P
HTT	6.037	23.45	8.232×10^{-9}	1.137
STT	7.004	26.4	6.594×10^{-9}	1.141
STC	4.578	33.45	4.634×10^{-8}	1.033

Table S2 Kinetic curves at 770 nm and the data fitted using multi-exponential decay components.

	A_1	τ_1(ps)	A_2	τ_2(ps)	A_3	τ_3(ps)	A_4	τ_4(ns)	A_5	τ_5(ns)
HTT	15%	4.5±1.0	15%	27±5.1	35%	209±27	-18%	0.44±0.12	17%	Long-lived
STT	-37%	1.8±0.4	--	--	--	--	-14%	0.38±0.11	49%	Decay
STC	22%	4.4±1.1	36%	69±6.2	--	--	--	--	42%	

References

1. G. H. Du, Q. Chen, P. D. Han, Y. Yu, L. M. Peng, Potassium Titanate Nanowires: Structure, Growth, and Optical Properties. *Phys. Rev. B* **2003**, *67*, 035323.
2. S. J. Clark, M. D. Segall, C. J. Pickard, P. J. Hasnip, M. J. Probert, K. Refon, M. C. Payne, First Principles Methods Using CASTEP. *Z. Kristallogr.* **2005**, *220,* 567.
3. D. M. Ceperley, B. J. Alder, Ground State of the Electron Gas by a Stochastic Method. *Phys. Rev. Lett.* **1980**, *45,* 566.
4. A. M. Rappe, K. M. Rabe, E. Kaxiras, J. D. Joannopoulos, Optimized Pseudopotentials. *Phys. Rev. B* **1990**, *41,* 1227.
5. H. J. Monkhorst, J. Pack, Special Points for Brillouin-Zone Integrations. *Phys. Rev. B* **1976**, *13,* 5188.